Correlation of anomalous write error rates and ferromagnetic resonance spectrum in spin-transfer-torque-magnetic-random-access-memory devices containing in-plane free layers

Eric R. Evarts, Ranko Heindl, William H. Rippard, and Matthew R. Pufall

Articles you may be interested in

Observations of thermally excited ferromagnetic resonance on spin torque oscillators having a perpendicularly magnetized free layer
J. Appl. Phys. **115**, 17C740 (2014); 10.1063/1.4868494

Low magnetisation alloys for in-plane spin transfer torque devices
J. Appl. Phys. **111**, 113904 (2012); 10.1063/1.4723824

Low writing energy and sub nanosecond spin torque transfer switching of in-plane magnetic tunnel junction for spin torque transfer random access memory
J. Appl. Phys. **109**, 07C720 (2011); 10.1063/1.3556784

Challenges toward gigabit-scale spin-transfer torque random access memory and beyond for normally off, green information technology infrastructure (Invited)
J. Appl. Phys. **109**, 07D325 (2011); 10.1063/1.3556681

Activation barriers of submicron magnetoresistive random access memory cells with single and synthetic antiferromagnet free layers
J. Appl. Phys. **99**, 08T317 (2006); 10.1063/1.2177050

Correlation of anomalous write error rates and ferromagnetic resonance spectrum in spin-transfer-torque-magnetic-random-access-memory devices containing in-plane free layers

Eric R. Evarts,[1] Ranko Heindl,[2] William H. Rippard,[1] and Matthew R. Pufall[1]

[1]*National Institute of Standards and Technology, 325 Broadway, Boulder, Colorado 80305, USA*
[2]*Department of Physics and Astronomy, San Jose State University, One Washington Square, San Jose, California 95192, USA*

In a small fraction of magnetic-tunnel-junction-based magnetic random-access memory devices with in-plane free layers, the write-error rates (WERs) are higher than expected on the basis of the macrospin or quasi-uniform magnetization reversal models. In devices with increased WERs, the product of effective resistance and area, tunneling magnetoresistance, and coercivity do not deviate from typical device properties. However, the field-swept, spin-torque, ferromagnetic resonance (FS-ST-FMR) spectra with an applied DC bias current deviate significantly for such devices. With a DC bias of 300 mV (producing 9.9×10^6 A/cm^2) or greater, these anomalous devices show an increase in the fraction of the power present in FS-ST-FMR modes corresponding to higher-order excitations of the free-layer magnetization. As much as 70% of the power is contained in higher-order modes compared to $\approx$20% in typical devices. Additionally, a shift in the uniform-mode resonant field that is correlated with the magnitude of the WER anomaly is detected at DC biases greater than 300 mV. These differences in the anomalous devices indicate a change in the micromagnetic resonant mode structure at high applied bias. © *2014 AIP Publishing LLC*. [http://dx.doi.org/10.1063/1.4879847]

Spin-transfer-torque (STT) magnetic random-access memory (MRAM) holds promise as a non-volatile, energy-efficient, high-speed memory.[1] In typical devices, the write-error rate (WER, defined as the number of non-switch events divided by the number of switching attempts) decreases exponentially with increasing pulse voltage. Anomalous devices exceed the usual exponential dependence of the WER on the pulse voltage, which limits usage of STT-MRAM.[2,3] While anomalous WERs are documented,[2,3] rapid identification of these anomalous devices has not been previously possible and the cause of the anomalies are not known. We present here a method for rapid identification of anomalous devices, using a signature in the device-level ferromagnetic resonance (FMR) spectrum. Once identified, anomalous devices can be carefully studied to understand the physics that leads to an increasing number of write errors, which is closely connected to the magnetization-reversal dynamics in the device.

The magnetization-reversal mechanism in STT devices is not well understood. From stroboscopic measurements involving time-resolved X-ray magnetic circular dichroism, previous researchers inferred that the reversal mechanism is dominated by the formation of a magnetic vortex in the nanomagnet.[4,5] Conversely, single-shot, real-time measurements of the resistance during the reversal of a STT device indicated that the device-reversal mechanism can be explained by coherent rotation.[6] Even with full micromagnetic simulations that include the STT effect, Aurélio *et al.* report that the magnetization reversal was dominated by the quasi-uniform magnetization reversal,[7] while Lee *et al.* report that the magnetization reversal was dominated by chaotic spin-wave excitation.[8] In all of the above cases, the magnetization fluctuations showed a dependence on the applied current density, which controls which regime the magnetization reversal will follow.

Field-swept spin-torque ferromagnetic resonance (FS-ST-FMR) has previously been used to understand the basic magnetic properties of magnetic tunnel-junction (MTJ) devices[9] and their use as diode detectors of microwaves.[10–12] This prior work analyzed only the single dominant resonance mode in the power spectrum at zero DC bias applied to the device. Here, analysis of the higher-order resonance modes gives meaningful information about the details of the magnetization oscillations in the device. These higher-order modes show a strong dependence on the applied DC bias in devices with an anomalous WER.

WER measurements were performed with the method presented by Heindl *et al.*[2] We attempted to switch each device $>10^6$ times to achieve WERs at the 10^{-6} level. We recorded the FS-ST-FMR spectra using an external magnetic field applied perpendicular to the plane of the device to within 1° and a measurement circuit with a bandwidth >30 GHz.[9] As the frequency was varied, the microwave power was adjusted so that constant power was delivered to the device.[9] Further experimental details of the FS-ST-FMR technique are described in Ref. 9. Spectra were recorded with a DC bias current. The currents were selected to give comparable current densities in different-sized devices to allow comparison between devices with different dimensions. For comparison with the WER results, we report the DC bias voltage at zero applied magnetic field with the device in the parallel state. When an external magnetic field is applied, the voltage measured across the device changes as the magnetizations of both the free layer and reference layer

are pulled out of the plane of the film. In this work, the highest-field resonant mode, which corresponds to the center or quasi-uniform resonant mode, will be referred to as the fundamental mode.[9,13] Measurements with FS-ST-FMR are reported here, due to the larger accessible frequency bandwidth; however, comparable results were also obtained with thermal FMR, where a DC bias is applied to the device and the power spectrum is recorded with a spectrum analyzer.

The devices reported here are representative samples of typical and anomalous devices from a single thin-film stack deposited as bottom electrode/PtMn 20.0 nm/ CoFe 2.5 nm/Ru 0.8 nm/CoFeB 2.5 nm/MgO 1.0 nm/ CoFeB 4.0 nm/Ta 10.0 nm/top electrode, and possess a resistance times area product (RA product) of $3\,\Omega$-μm^2, a tunneling magnetoresistance (TMR) of 70%, and a nominal STT quasi-DC switching voltage of 0.4 V. The devices were patterned into elliptical nanopillars down to the MgO tunnel barrier via argon-ion milling. The devices ranged in size from 50 nm × 150 nm to 70 nm × 210 nm. The representative typical (anomalous) device whose properties are discussed in Figs. 1–3 is 60 nm × 180 nm (50 nm × 150 nm). We measured more than 20 elliptical devices from seven different thin-film stacks. The films are qualitatively similar to this representative film, with minor variations in layer thickness or deposition parameters. These additional films all show the same trends, as discussed here for specific cases.
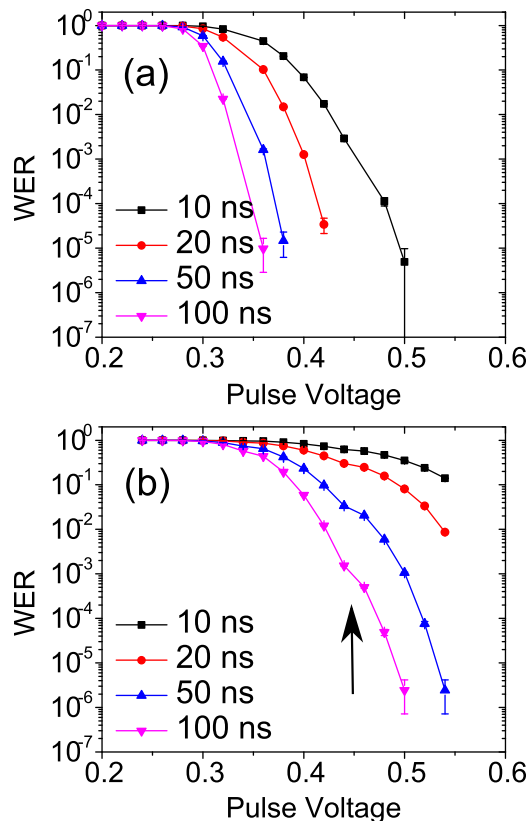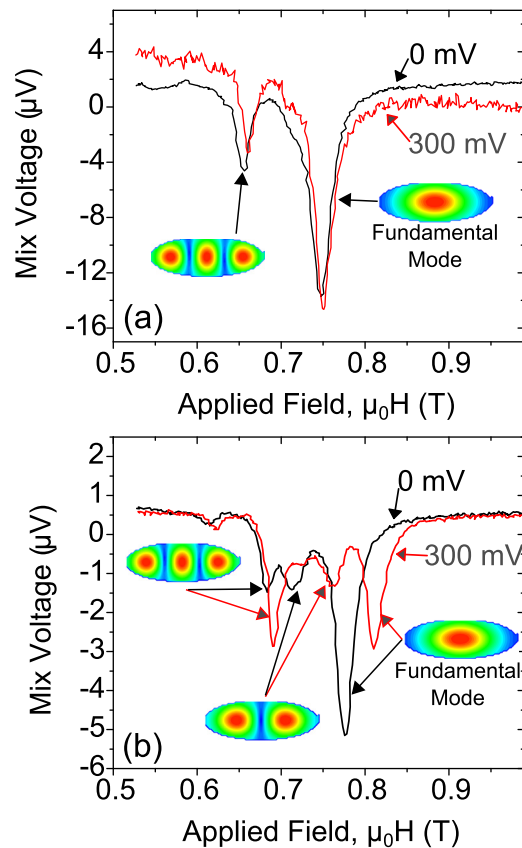

FIG. 2. (a) Representative typical device FS-ST-FMR spectra acquired at 15 GHz for a 60 nm × 180 nm device. The spectra at 0 mV (black) and 300 mV (9.9×10^6 A/cm^2) (red) DC bias show no significant differences. (b) Representative anomalous device FS-ST-FMR spectra at 15 GHz for a 50 nm × 150 nm device. As the DC bias is increased from 0 mV (black) to 300 mV (9.9×10^6 A/cm^2) (red), power shifts from the fundamental mode to one of the higher-order modes. Simultaneously, the resonant field of the modes increases. The shape of the modes corresponding to these resonances has been determined from micromagnetic simulations through the method of McMichael and Stiles.[13]

FIG. 1. (a) WER as a function of pulse voltage and pulse duration for the representative typical device with lateral dimensions of 60 nm × 180 nm. (b) WER as a function of pulse voltage and pulse duration for the representative anomalous device with lateral dimensions of 50 nm × 150 nm. In this plot, the anomaly is visible at 0.44 V (arrow).

WERs as a function of pulse amplitude and pulse duration, for the representative typical and anomalous devices, are shown in Figs. 1(a) and 1(b), respectively. In a macrospin model,[2] the WER at fixed pulse duration should decrease exponentially as the pulse amplitude increases. The amplitude required to achieve a given WER should decrease as the pulse duration increases. However, for a fixed pulse duration, anomalous devices deviate from the expected exponential decrease in WER as the pulse amplitude increases. This deviation appears as a kink in the WER as the pulse amplitude increases. This kink appears at the same pulse amplitude, independent of the pulse duration (at 0.44 V in Fig. 1(b)). The apparent magnitude of this WER anomaly varies from device to device; however, quantification of the anomaly from WER measurements is very time-consuming. Below we describe a faster, alternative method.

Quasi-static switching measurements of both typical and anomalous devices of any size indicate no significant differences. For this representative film, we report quasi-static results from five typical devices and five anomalous devices with both WER and FS-ST-FMR data. The effective RA product of the parallel resistance state for the typical devices
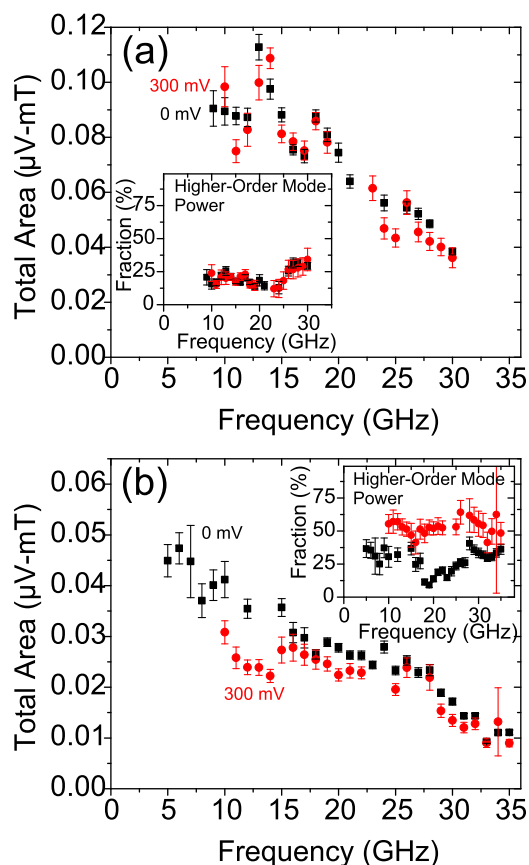
FIG. 3. (a) For the representative typical device with lateral dimensions of 60 nm × 180 nm, the sum of areas under all fitted peaks in the FS-ST-FMR spectra at 0 mV (black square) and 300 mV (9.9×10^6 A/cm^2) (red circle). No change in total area is observed with increasing DC bias. Inset: the fraction of power in higher-order modes does not change with increasing DC bias. (b) In the representative anomalous device with lateral dimensions of 50 nm × 150 nm, no significant change in the sum of areas under all fitted peaks in the FS-ST-FMR spectra at 0 mV (black square) and 300 mV (9.9×10^6 A/cm^2) (red circle). The slight decrease in the 300 mV area in this particular device is not seen in all anomalous devices. Inset: As the DC bias is increased, a significant increase in the fraction of power in higher-order modes is observed at all frequencies. Error bars are calculated from the error on the amplitude fits of the resonance peaks and indicate 2σ error.

is 3.2 Ω-μm^2 ± 0.2 Ω-μm^2 and for the anomalous devices is 3.0 Ω-μm^2 ± 0.4 Ω-μm^2 for devices on the film presented here. Here, the TMR is 65% ± 7% and 60% ± 9% for typical and anomalous devices, respectively. The measured coercivity ($\mu_0 H_c$) of each device is consistent with the average coercivity of devices of the given size on this thin film with values ranging over 10 mT to 20 mT. The lack of discernible differences in the quasi-static properties of typical and anomalous devices suggests that the devices do not deviate significantly from the expected size or shape, and that the thin-film stack appears to have no significant variation of tunnel-barrier thickness, tunnel-barrier crystallographic orientation, or magnetic anisotropy (derived from quasistatic device measurements).

Interestingly, at zero applied DC bias current, the typical device and anomalous device FS-ST-FMR spectra are qualitatively similar, with a prominent fundamental resonance mode and much smaller higher-order modes, as seen in Fig. 2 for a single frequency. The number of visible resonance peaks varies from device to device and is not correlated with its size or whether a particular device is typical or

anomalous. However, under application of a bias, there is a correlation between the quantitative behavior of a device's resonance modes and the device behavior. When a DC bias is applied during the FS-ST-FMR measurements, there is no change (within measurement error) in the resonant fields, amplitudes, or line widths extracted from typical device spectra. In anomalous devices, however, there are two changes in the spectra: (1) a shift of power from the fundamental mode into one of the higher-order (lower-field) modes and (2) a shift of the resonant field of the fundamental mode toward higher field with increasing DC bias current above a threshold current.

As the DC bias is increased, there is no systematic change in the total resonance absorption measured in the device, as shown in Fig. 3 for the representative devices. In Fig. 3(b), the discrepancy in this particular anomalous device between the 0 mV and 300 mV (9.9×10^6 A/cm^2) total peak area is not seen in all anomalous devices. The decrease in total power, as the frequency increases, is due to a combination of the free-layer magnetization stiffening with the increasing applied external field and the fixed layer starting to rotate out of the plane of the film.

In typical devices, the fraction of power detected in higher-order modes is constant with frequency and bias (Fig. 3(a) inset for the representative typical device). In anomalous devices, while the fraction of power in higher-order modes is still approximately constant with frequency, there is an increase in the power detected in higher-order modes at 300 mV, as compared to 0 mV (Fig. 3(b) inset for the representative anomalous device). In anomalous devices, as much as 70% of the power is detected in the higher-order modes when 300 mV DC bias is applied. In Fig. 3, the powers from all higher-order modes are summed together for simplicity. However, the particular mode with the largest relative amplitude changes from device to device, and as a function of frequency in the same device.

In anomalous devices, the resonant fields of all observed modes increase with the magnitude of the applied DC bias, as seen for the representative anomalous device in Fig. 2(b). The shift towards higher resonant fields is equivalent to shifting towards lower resonant frequency. This resonant field shift appears only above a threshold DC bias, usually between 200 mV (6.6×10^6 A/cm^2) and 300 mV. In typical devices, the resonant fields of the observed modes do not shift with applied DC biases up to 400 mV (13×10^6 A/cm^2). The magnitude of the resonant-field shift is proportional to the prominence of the WER anomaly and potentially allows quantification of the WER anomaly with a simple measurement. In devices having a barely-discernible WER anomaly, a small resonant field shift of a few millitesla is detected at 400 mV DC bias. With a prominent WER anomaly, resonant field shifts as large as 40 mT at 400 mV DC bias occur. At biases greater than 400 mV, most devices underwent tunnel-barrier breakdown during the prolonged application of the bias during FS-ST-FMR measurements for the film discussed here.

The resonant field is determined by the net effective field seen by the free layer of the device, which is dominated by the sum of the demagnetizing field, the anisotropy field, the exchange field, and the external applied field. For the

currents applied here, we estimate the Oersted field to exhibit approximately 1 mT field difference between the ends of the devices, which can be safely ignored. As the current density increases, the resonant field should decrease, because the magnitude of the STT effect will increase, which decreases the effective demagnetizing field by increasing the cone angle of the oscillation.[14] A field-like STT-effect component will appear as an effective increase in the external applied field, which would also lead to a decrease in the resonance field. Another potential source of a resonant-field shift is from voltage-controlled anisotropy. However, with voltage-controlled anisotropy, there should be a linear dependence on the applied voltage, which is contrary to the shift towards increasing resonant fields for both signs of the applied voltage observed here.[15,16] As power shifts out of the fundamental mode, the opening angle should decrease, which would lead to an increase in the effective demagnetizing field and an increase in the resonant field. This cannot, however, explain the increase in the resonant field in the higher-order modes as more power flows into those modes. There must be additional changes in the structure of the modes to produce an increase in the resonant fields, as shown in these data.

The FS-ST-FMR measurements are performed with the magnetic field perpendicular to the film plane with the magnetization of the free layer saturated in this direction. During pulsed switching measurements, the free-layer magnetization lies within the plane of the film. In a macrospin model or coherent in-plane rotation model, the magnetization will not pass through the geometry of the FS-ST-FMR measurement. However, from the presence of higher-order modes, we determined that the magnetization is not following these simple models. From micromagnetic simulations, for the vortex state, domain-wall-propagation, and chaotic reversal mechanisms,[5,7,8] some parts of the magnetization during switching should pass through the perpendicular orientation used in the FS-ST-FMR technique. The shift of power from the fundamental mode into a higher-order mode indicates increased non-uniform magnetization oscillation in anomalous devices compared to typical devices that could impede coherent rotation and rule out any approximations as quasiuniform or macrospin-based models. A shift of power at non-zero DC bias suggests that the power shift is not due to physical defects alone, since these defects should also appear in the zero-DC-bias case, but requires the additional energy from both the Oersted field produced by the charge current and the torque on the magnetization from the STT effect.

We have shown a correlation between a spectral signature from FS-ST-FMR measurements and the anomalous WERs in MRAM devices with in-plane free layers. This spectral signature allows rapid identification of anomalous devices. Anomalous devices inject a larger fraction of the total power into higher-order modes when a DC bias is applied. As much as 70% of the total power is contained in these higher-order modes, compared to approximately 20% of the total power in typical devices. Above a threshold bias, anomalous devices show a shift in the resonance fields that indicate a change in the details of the mode structure and coupling that cannot be precisely determined from these data.

[1]B. N. Engel, J. Akerman, B. Butcher, R. W. Dave, M. DeHerrera, M. Durlam, G. Grynkewich, J. Janesky, S. V. Pietambaram, N. D. Rizzo, J. M. Slaughter, K. Smith, J. J. Sun, and S. Tehrani, IEEE Trans. Magn. **41**, 132 (2005).

[2]R. Heindl, W. H. Rippard, S. E. Russek, and A. B. Kos, Phys. Rev. B **83**, 054430 (2011).

[3]T. Min, Q. Chen, R. Beach, G. Jan, C. Horng, W. Kula, T. Torng, R. Tong, T. Zhong, D. Tang, P. Wang, M. Chen, J. Z. Sun, J. K. Debrosse, D. C. Worledge, T. M. Maffitt, and W. J. Gallagher, IEEE Trans. Magn. **46**, 2322 (2010).

[4]Y. Acremann, J. P. Strachan, V. Chembrolu, S. D. Andrews, T. Tyliszczak, J. A. Katine, M. J. Carey, B. M. Clemens, H. C. Siegmann, and J. Stöhr, Phys. Rev. Lett. **96**, 217202 (2006).

[5]J. P. Strachan, V. Chembrolu, Y. Acremann, X. W. Yu, A. A. Tulapurkar, T. Tyliszczak, J. A. Katine, M. J. Carey, M. R. Scheinfein, H. C. Siegmann, and J. Stöhr, Phys. Rev. Lett. **100**, 247201 (2008).

[6]Y.-T. Cui, G. Finocchio, C. Wang, J. A. Katine, R. A. Buhrman, and D. C. Ralph, Phys. Rev. Lett. **104**, 097201 (2010).

[7]D. Aurélio, L. Torres, and G. Finocchio, J. Appl. Phys. **108**, 083911 (2010).

[8]K.-J. Lee, A. Deac, O. Redon, J.-P. Nozières, and B. Dieny, Nature Mater. **3**, 877 (2004).

[9]E. R. Evarts, M. R. Pufall, and W. H. Rippard, J. Appl. Phys. **113**, 083903 (2013).

[10]A. A. Tulapurkar, Y. Suzuki, A. Fukushima, H. Kubota, H. Maehara, K. Tsunekawa, D. D. Djayaprawira, N. Watanabe, and S. Yuasa, Nature **438**, 339 (2005).

[11]H. Kubota, A. Fukushima, K. Yakushiji, T. Nagahama, S. Yuasa, K. Ando, H. Maehara, Y. Nagamine, K. Tsunekawa, D. D. Djayaprawira, N. Watanabe, and Y. Suzuki, Nat. Phys. **4**, 37 (2008).

[12]D. Bang, T. Taniguchi, H. Kubota, T. Yorozu, H. Imamura, K. Yakushiji, A. Fukushima, S. Yuasa, and K. Ando, J. Appl. Phys. **111**, 07C917 (2012).

[13]R. D. McMichael and M. D. Stiles, J. Appl. Phys. **97**, 10J901 (2005).

[14]W. H. Rippard, M. R. Pufall, and S. E. Russek, Phys. Rev. B **74**, 224409 (2006).

[15]T. Nozaki, Y. Shiota, M. Shiraishi, T. Shinjo, and Y. Suzuki, Appl. Phys. Lett. **96**, 022506 (2010).

[16]M. Weiler, A. Brandlmaier, S. Geprägs, M. Althammer, M. Opel, C. Bihler, H. Huebl, M. S. Brandt, R. Gross, and S. T. B. Goennenwein, New J. Phys. **11**, 013021 (2009).